PIXE analysis of historical paintings: Is the gain worth the risk?

ARTICLE *in* NUCLEAR INSTRUMENTS AND METHODS IN PHYSICS RESEARCH SECTION B BEAM INTERACTIONS WITH MATERIALS AND ATOMS · AUGUST 2015

Impact Factor: 1.12 · DOI: 10.1016/j.nimb.2015.08.072

3 AUTHORS:

Thomas Calligaro

Centre de Recherche et de Restauration de…

94 PUBLICATIONS **1,180** CITATIONS

SEE PROFILE

Victor Gonzalez

Ministère de la culture et de la communicat…

3 PUBLICATIONS **0** CITATIONS

SEE PROFILE

Laurent Pichon

Centre de recherche et de restauration des …

44 PUBLICATIONS **340** CITATIONS

SEE PROFILE

Nuclear Instruments and Methods in Physics Research B xxx (2015) xxx–xxx

Contents lists available at ScienceDirect

Nuclear Instruments and Methods in Physics Research B

journal homepage: www.elsevier.com/locate/nimb

PIXE analysis of historical paintings: Is the gain worth the risk?

T. Calligaro [a,b,c,*], V. Gonzalez [a,b], L. Pichon [a,c]

[a] Centre de recherche et de restauration des musées de France, C2RMF, Palais du Louvre – Porte des Lions, 14 Quai François Mitterrand, 75001 Paris, France
[b] PSL Research University, Chimie ParisTech – CNRS, Institut de Recherche Chimie Paris, UMR8247, 75005 Paris, France
[c] Fédération de recherche NewAGLAE, FR3506 CNRS – Ministère de la Culture – IRCP, Palais du Louvre, 75001 Paris, France

ARTICLE INFO

Article history:
Received 15 March 2015
Received in revised form 26 August 2015
Accepted 26 August 2015
Available online xxxx

Keywords:
PIXE
Imaging
Paintings
Lead white
Damage

ABSTRACT

The PIXE analysis of easel paintings constitutes a challenging task. Despite recognized merits and a few emblematic applications, PIXE has never been routinely applied to these fragile, complex and precious targets. The present work discusses the place of PIXE in the study of easel paintings and opens up perspectives for a more systematic usage of this analytical technique. Progress achieved since decades in the implementation of PIXE to study such fragile cultural heritage artefacts is reviewed, notably at the LABEC laboratory in Italy and at the AGLAE facility of the C2RMF in France. Two specific techniques developed for paintings are detailed and exemplified on Renaissance painting masterpieces: differential PIXE for paint layers depth profiling and multi-scale elemental mapping for the imaging of pigment distribution. Beam-induced damage, a major concern, notably depends on the employed beam fluence in particle/cm^2 or μC/cm^2. After recalling previous works on damage induced in chemical products comparable to pigments, we present the behaviour under different fluences of protons of a few MeV (1–300 μC/cm^2) of targets having high resemblance to historical easel paintings: pellets of specially synthesized lead white pigments, layers of lead white mixed with linseed oil and areas containing lead white of two 19th century paintworks. The results shed new lights on the behaviour of paintworks under the beam and pave the way to strategies for damage mitigation. In particular, the lowering of PIXE performance induced by the decrease of the beam fluence sets a trade-off between risk of damage and gained information which also impacts the PIXE scanning protocol for paintings. As an illustration of an adequate adjustment of this balance, we report the exploratory application of PIXE mapping to a large area of a 19th century easel painting without damage. The recorded elemental maps are compared to elemental maps collected on the same area using laboratory-based scanning XRF.

1. Background and stakes

The direct chemical analysis of easel paintings in view to identify paint materials and to understand the artist's creation technique is a quite challenging task. Firstly because paintworks are complex objects consisting of a stack of many paint layers of several tens of microns thick, each containing various mineral pigment grains dispersed in an organic binder. Paint layers are applied on a preparation substrate (primer) previously deposited on the support (canvas or wood) and covered by tens of micrometers of varnish. The second reason is that the techniques that are suitable for the analysis of such fragile and irreplaceable works have to comply with strong non-destructive and non-invasive criteria. Surprisingly, whereas cultural heritage has always been a very active application field of PIXE [1,2], few works have addressed the direct analysis of easel paintings. This can be ascribed to a perceived risk of beam damage that exceeds the potential gain of information. Indeed, even when an access to a particle accelerator is available, as it is the case at the C2RMF, X-ray fluorescence (XRF) generally remains the preferred analytical method, considered as safe as radiography and providing satisfactory results. Nevertheless, PIXE possesses intrinsic qualities that can make it unique and attractive for the study of paintworks provided non-damaging operating conditions can be insured. As a matter of fact, if PIXE bears similarities with XRF, the use of protons instead of X-rays as a probing radiation confers to this method attractive features for painting studies, such as an analysed depth controlled by the energy of the particle beam and an improved yield for light elements.

* Corresponding author at: Centre de recherche et de restauration des musées de France, C2RMF, Palais du Louvre – Porte des Lions, 14 Quai François Mitterrand, 75001 Paris, France.

http://dx.doi.org/10.1016/j.nimb.2015.08.072
0168-583X/

2. PIXE analysis of paintworks: developments and applications

The direct analysis of easel paintings by PIXE has provided a strong impetus to the development of external beams, since the large dimensions of these artefacts and their heterogeneous and fragile nature preclude their placement in a vacuum chamber. Many methodological improvements in external beam end-stations and in the IBA implementation in air were achieved in laboratories dedicated to the study of cultural heritage relics, e.g. at the LABEC in Florence, Italy [3,4] and at the C2RMF in Paris, France [5,6]. As a consequence, a vast panel of IBA techniques can now be applied at atmospheric pressure with performances approaching those obtained under vacuum [7]. As an illustration of the vitality of this research field, two specific techniques targeting easel paintings are described hereafter, namely differential PIXE and multi-scale PIXE mapping.

2.1. Differential PIXE

The differential PIXE technique was developed to determine in a direct and non-destructive way the paint layer composition and ordering, a task usually achieved by examining cross-sections sampled in paintings by means of SEM-EDX. The principle of differential PIXE relies on the recording of PIXE spectra at increasing beam energies (e.g. 1, 2, 3 and 4 MeV) whose progressive penetration induces the excitation of deeper and deeper layers. The comparison of the spectra allows to deduct the depth profiles of the paint layer stack. The theoretical grounds of this technique were early established [8] and tested on artificial paint layer sequences [9,10]. One of the first applications of differential PIXE to a historical painting was a dual energy study at 2 and 4 MeV of the "Christus und Maria Magdalena" attributed to Cranach the Elder (1515–1520) [11]. Differential PIXE was extensively developed at the LABEC [12,13] and applied to Renaissance masterpieces, e.g. the "Madonna dei fusi" attributed to Leonardo da Vinci (1501) [14] or the "Santa Lucia" painted by Giorgio Vasari (1567) [15]. The layer reconstruction algorithms were improved by Smit and coworkers to include light elements (e.g. binders) and applied to the "Street in Munich" painted by Matej Sternen [16]. An alternative to differential PIXE is PIXE under variable incident angle, but its implementation was found more complex [17].

The combined use of external beam PIXE and RBS using a single proton irradiation was another approach early suggested, but the need of a high beam energy resolution on the target for RBS postponed this solution till the introduction of the ultrathin beam exit window [18,19]. The PIXE/RBS coupling has been employed to determine pigment composition and to estimate organic to binder ratio in Italian Renaissance paintworks [20]. The RBS and PIXE spectra of paint layers can be processed separately using GUPIX and SIMNRA programs or in a simultaneous and self-consistent way using specific codes such as Data Furnace, as demonstrated by Beck and co-workers [21,22]. This promising coupled PIXE/RBS approach could probably be generalized to interpret differential PIXE measurements. A survey of the various techniques based on PIXE for the non-destructive characterisation of paint layers (differential PIXE, line intensities ratios such as K_α/K_β, variable angle PIXE and combination with RBS) was published in the framework of the European COST G1 action [23–25].

The paint layer compositions and thicknesses derived using differential PIXE (and with the other techniques) are generally considered as qualitative only. In fact, the relative imprecision of the reconstructed layers does less stem from the method itself or from the experiment than from the intrinsic heterogeneity of the paint layers which vary from point to point, thus notably departing from the hypothesized parallel layer model.

2.2. Multiscale PIXE mapping

The chemical imaging of easel paintings is particularly useful to identify pigments by means of their elemental composition and to map their spatial distribution, revealing the painter's palette and the way the artist has created its composition. A review by Alfeld and co-workers clearly showed the great benefit of comparing elemental maps with pictures recorded using various imaging techniques: visible photography, UV fluorescence imaging, IR reflectrography, X-ray radiography, X-ray laminography, etc. [26]. As already mentioned, the usual technique employed to identify non-destructively pigments in painting by means of their elemental composition is XRF, because of its simplicity and safety. Derived from the synchrotron, the scanning macro XRF imaging technique (MA-XRF) generalize this approach to an area of the painting by drawing elemental maps moving pixel by pixel the XRF spectrometer in front of the work [27]. MA-XRF is rapidly progressing but still requires hours to days for the acquisition of full maps [28]. Even if point analysis remains the routine technique for paintings, this method that can be qualified as 'colour radiography' is increasingly employed since it enables a new vision of paintings, often disclosing unexpected features. External beam PIXE can also be employed for this task, with two advantages compared to MA-XRF: an increased X-ray production yield for elements of low atomic number and a rapid scanning of the proton beam using magnetic deflection. In external beams, the extension of the raster scanned area is limited by the size of the exit window aperture (few millimetres). To scan larger areas, the painting is mechanically moved in front of the external beam using a motorised easel [29]. Remarkable examples of multiscale PIXE mapping were achieved at the LABEC, such as the "Madonna col Bambino" by Andrea Mantegna, 1460 [30] and the "Ritratto Trivulzio" by Antonello da Messina (1476) [31]. In the former, elementals maps allowed to evidenced a palette containing lead white ($PbCO_3$/$Pb_3C_2O_8H_2$), gold powder, lead–tin yellow (Pb_2SnO_4), ultramarine ($Na_3CaAl_3Si_3O_{12}S_4$) in the eye and the veil of the Virgin. In the latter, the meticulous interpretation of centimetre-sized maps including light elements such as Al, K and Ca, and the combination with differential PIXE measurement allowed to identify the pigments (cinnabar, red lake with potash alum mordent, lime preparation) and provided information on layer ordering.

3. Damage in pigments and paint layers

Radiation-based analytical techniques are reputed harmless for the studied sample, and this is one reason of the success of these methods in the field of cultural heritage. However, as underlined by Bertrand and co-workers in a recent survey, the use of high ion or photons fluxes produced by particle accelerators, synchrotrons or lasers can induce modifications in the most fragile materials and motivate the development of damage mitigation strategies (Ref. [32] and herein). In the present case, the major concern is the possible modification induced by the proton beam in paint materials such as varnish, binders and pigments, notably lead white that was employed from Antiquity to the 19th c. In a comprehensive review, Zucchiatti and Agulló-Lopez have explored the potential consequences of ion beam damage induced during ion beam analysis of cultural heritage materials [33]. The authors considered damage mechanisms occurring under a wide range of irradiation conditions: different ion beams (protons, helium and heavier ions) of 1–30 MeV, intensities from 0.1 to 10 nA, beam size from 50 μm to 1 mm, fluences between 10^{13} and 10^{16} particle/cm^2. The damage regimes that prevail for different ions at different velocities were considered, as well as the potentially induced effects including darkening by colour centre formation, target

Please cite this article in press as: T. Calligaro et al., PIXE analysis of historical paintings: Is the gain worth the risk?, Nucl. Instr. Meth. B (2015), http://dx.doi.org/10.1016/j.nimb.2015.08.072

heating, mobilisation of target atoms, incident ions implantation and eventually sputtering of target atoms by heavy ion beams. In addition, the authors reported the beam fluences employed in the previous PIXE studies of historical paintings, which varied from 1 to 3 10^{13} protons/cm^2 (1.6–5 μC/cm^2) depending on the beam size. Investigations on beam induced damage initially focused on white pigments where alteration marks can be more easily observed. The first works addressed the sensitivity of hydrocerussite $2PbCO_3{\cdot}Pb(OH)_2$, one of the two main constituents of lead white. Absil and co-workers found that the dark marks induced by beam fluences of 10^{15} protons/cm^2 were not accompanied by a measurable structural or molecular modification using XRD and Raman spectrometry [34]. Darkening was ascribed to the formation of colour centres on the basis of electron paramagnetic resonance and thermoluminescence measurements, a conclusion supported by the observed reversibility of the stain under UV illumination and moderate heating. Enguita and co-workers confirmed the production of colour centres in various pigments, including cerussite ($PbCO_3$), the other constituting phase of lead white [35]. Beck and co-workers have pursued the study of lead white and extended it to other white pigments: titanium white (TiO_2), which was found almost insensitive to the beam, calcite ($CaCO_3$), zinc white (ZnO), gypsum ($CaSO_4$), lead sulphate ($PbSO_4$) and lithopone ($BaSO_4$ and ZnS) which were moderately marked compared to lead white which is the most prone to alteration [36]. The optical density of the mark in lead white was estimated and its reversible character when induced under moderate fluence was confirmed. On the other hand, when exploring the effect of high fluences (10^{17} protons/cm^2) corresponding to a fixed 50-μm external microbeam on lead white, structural modifications were evidenced by the reduction of the symmetric C-O stretching bands at 1050 cm^{-1} in the Raman spectrum and the modifications in the X-ray photoelectron spectrum of 1s levels of carbon and oxygen.

These previous studies have demonstrated that white pigments are not equally affected by irradiation with protons, lead white being the most sensitive one with a damage strongly depending on the beam intensity. However, to provide useful guidelines for a safe PIXE analysis of paintworks, damage should be investigated under realistic irradiation conditions. Among the different IBA methods, PIXE is the one requiring the less intense beam (less than 1 nA). For beam-induced modifications beam in the low intensity regime, the relevant physical quantity is the fluence, i.e. the total number of protons per unit area that has impacted the sample expressed in protons/cm^2 or more conveniently in μC/cm^2. In this study, three regimes are considered: the low fluence (below 10 μC/cm^2), the intermediate fluence (10–40 μC/cm^2), and the high fluence (above 40 μC/cm^2). Such apparently high values should not be misleading, as in proportion using a millimetre beam they correspond to moderate intensities (e.g. a 10-μC/cm^2 fluence corresponds to an irradiation with a 1-mm^2 diameter beam of 1 nA during 100 s).

The studied materials should also reflect as closely as possible those employed in historical paintings. For instance, lead white used by painters contains both hydrocerussite and cerussite crystals in variable proportion [37]. Prior the advent of industrial processes in the mid 19th century, this pigment was obtained from the so-called 'Dutch' or 'Stack' method where metallic lead sheets were exposed to vinegar fumes in a carbon dioxide atmosphere emanating from horse manure. The progressive transformation of metallic lead into lead acetate and further into lead carbonates yielded a white powder containing both mineral phases with variable crystal sizes [38]. After being finely ground and washed, the painter mixed the pigment powder with an organic binder, either lipid (e.g. linseed oil) or protein (e.g. egg white) with an approximately 20:1 weight ratio to make a preparation suitable for painting. The damage induced by a proton beam in this heterogeneous mixture has, to our knowledge, not been investigated.

4. Experimental and results

We present here the results obtained on three paint materials having more and more resemblance to easel paintings. The first consists of pure hydrocerussite and cerussite powder pellets specially synthesized at different crystal growths that were exposed to protons beams having 1, 2, 3 and 4 MeV to evaluate the effect of mineral phases and crystal sizes and to search for molecular modifications. Colour modifications were quantified in CIE L^*a^*b coordinates using fibre optical reflectance spectrocolorimetry (STIL model Ruby), electronic defects were characterised by electron paramagnetic resonance spectroscopy (Bruker Elexsys E500). Molecular modifications were investigated using μ-Raman spectroscopy (Renishaw Invia) and structural changes using a prototype μ-XRD diffractometer (OSMIC microfocused source producing a 200-μm parallel Cu Kα X-ray beam combined with a Rigaku R-AXIS IV++ imaging plate). The second paint materials were model paint layers made of 120-μm thick layers of a mixture of lead white with linseed oil that were exposed to low fluences of 3-MeV protons. Damage was investigated using the same protocol as for the pellets and mechanical deformations of the paint layer were measured using 3D digital microscopy (HIROX model KH7700). Lastly, the behaviour under the beam of areas painted with lead white in two 19th century portraits acquired by the C2RMF for testing purposes was observed. The aim was to explore the low fluence domain where damage starts to appear and to record the first signs of alteration. The irradiation was carried out using the New AGLAE scanning system [39] that provides a homogeneous repartition of the beam charge over 3 × 3 mm^2 areas that are required for spectrocolorimetric measurements.

4.1. Lead white crystalline phases

In order to investigate the influence of the crystallite size on damage sensitivity, cerussite and hydrocerussite were synthesized under pH controlled aqueous conditions. As shown in Fig. 1, immediately after synthesis cerussite crystallites (C_0) are needle-shaped (length ~1 μm) and hydrocerussite crystallites (H_0) are hexagonal platelet-shaped (size ~0.2 μm). After 15 days of crystal growth, cerussite (C_{15}) particles lose their needle shape and present a more massive aspect (up to ~5 μm), they are accompanied by small rhombohedric crystallites, while hydrocerussite (H_{15}) platelets remain hexagonal and grow up to ~5 μm.

The visual modifications were evaluated using the Euclidian distance between the measured CIE L^*a^*b colour coordinates on the phases, $\Delta E = \sqrt{\{(\Delta L^*)^2 + (\Delta a^*)^2 + (\Delta b^*)^2\}}$. In the CIE system, introduced to reflect the human eye perception, 1–2 units correspond to the smallest noticeable visual change. As shown in Table 1, irradiation with 3-MeV protons at high fluences (380 μC/cm^2) induced a comparable colour change in C_0 ($\Delta E = 16.9$) and H_0 ($\Delta E = 16.6$). However, H_{15} obtained after crystal growth was found much more sensitive to irradiation than H_0 ($\Delta E = 33.1$) and than C_{15} ($\Delta E = 9.6$). In addition, an intense ionoluminescence under the proton beam, previously reported [35], was recorded for cerussite, but not for hydrocerussite. No molecular or structural change could be evidenced by Raman spectrometry or XRD under these conditions. Alternatively the EPR spectra recorded on irradiated cerussite (C) and hydrocerussite (HC) are complex, and consist in the superposition of at least two species. Their g-factor is very close to the free spin value $g = 2.002$, which eliminates paramagnetic states of transition metal impurities. The nearly isotropic central

Please cite this article in press as: T. Calligaro et al., PIXE analysis of historical paintings: Is the gain worth the risk?, Nucl. Instr. Meth. B (2015), http://dx.doi.org/10.1016/j.nimb.2015.08.072

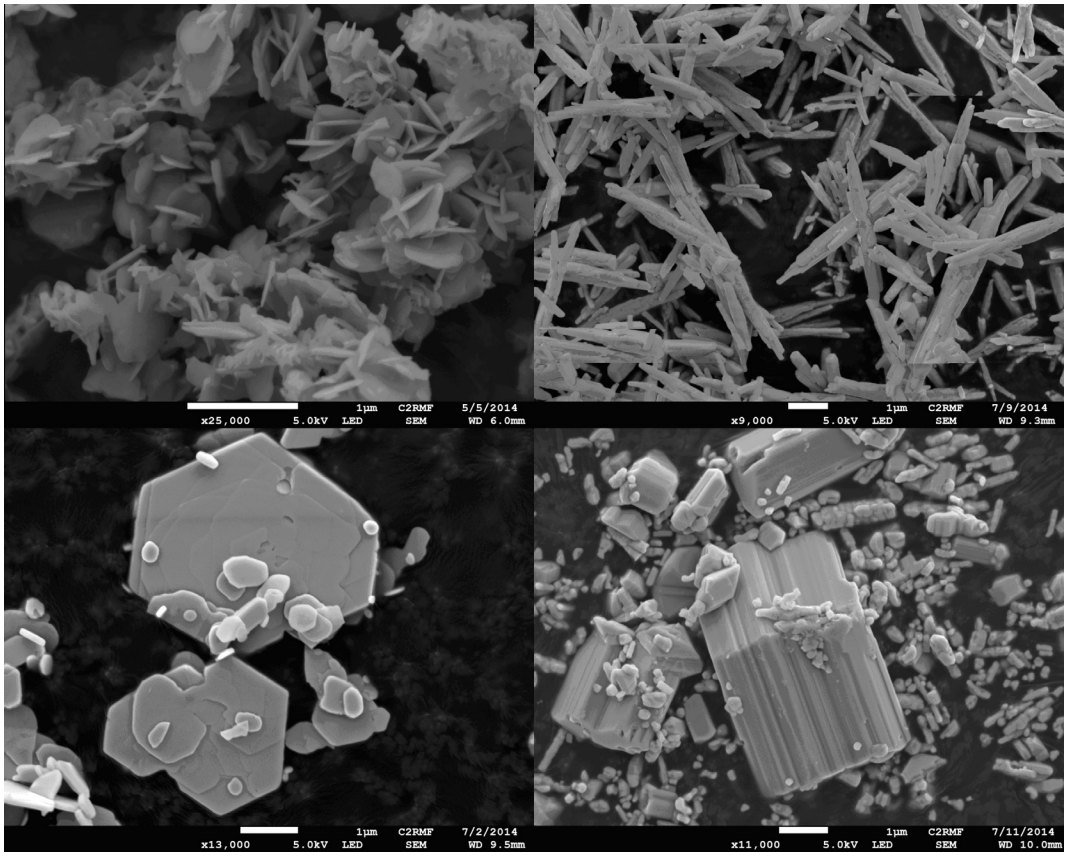

Fig. 1. SEM images of cerussite (left) and hydrocerussite (right) crystals, immediately after synthesis (top) and after 15 days of crystal growth (down).

Table 1
CIE $L^*a^*b^*$ colour coordinates of the two main phases of lead white with different crystallite size before and after irradiation with a high fluence. Hydrocerussite, in particular H_{15}, is the most prone to damage.

	Prior irradiation			After irradiation at 380 μC/cm^2		
	L^*	a^*	b^*	L^*	a^*	b^*
C_0	96.0	−1.8	3.6	88.4	−0.6	18.6
C_{15}	95.8	−1.0	7.0	92.5	−1.3	16.0
H_0	93.8	−2.3	6.0	85.4	−0.6	20.2
H_{15}	94.1	−0.4	7.4	61.3	1.3	11.8

line of C and HC, which is stable more than one month after irradiation, is ascribed to a defect at carbonate anion site (Fig. 2).

The crystalline nature of lead white appeared to play a key role in its sensitivity to damage. Hydrocerussite was found to be the most fragile phase with a sensitivity dramatically that depends on crystallite size. Because hydrocerussite to cerussite proportion and crystallite size in lead white vary from one painting to another, pigment sensitivity is hardly predictable. Let us recall that these worrisome results were obtained at intermediate or high fluences and, as will be shown in the next section, the situation at low fluence is more reassuring.

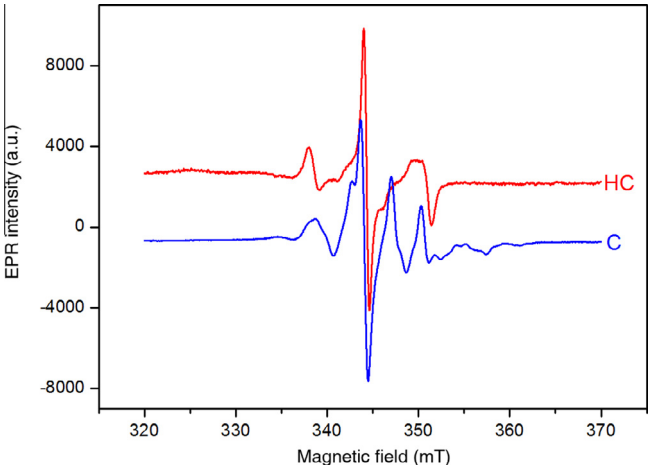

Fig. 2. EPR spectra recorded at 9 GHz for hydrocerussite (HC) and cerussite (C) after irradiation at 380 μC/cm^2. The nearly isotropic central line for C and HC, which is stable more than one month after irradiation, is due to a defect at carbonate anion site.

4.2. Model paint layers

Samples representative of a traditional lead white-based paint layer were elaborated from a cerussite/hydrocerussite pigment powder (Kremsweiss 70% HC/30% C mixture from Kremer Pigmente) mixed with linseed oil in proportions used in paintings (20:1 in weight). The paint material was applied on microscope glass slide with a thickness of 120 μm using a paint film applicator (ERICHSEN GmbH model 360-13) that fits the range of protons up to 4 MeV. Irradiation with intermediate fluences of protons of 2, 3 and 4 MeV induced a very similar brownish mark, suggesting that damage cannot be avoided using different proton beam energy. It was noted that the maximum damage occurred at the end of the range, as can be noted on the picture taken from the back of the slide (Fig. 3). Beam damage induced in-depth of the paintwork

Please cite this article in press as: T. Calligaro et al., PIXE analysis of historical paintings: Is the gain worth the risk?, Nucl. Instr. Meth. B (2015), http://dx.doi.org/10.1016/j.nimb.2015.08.072

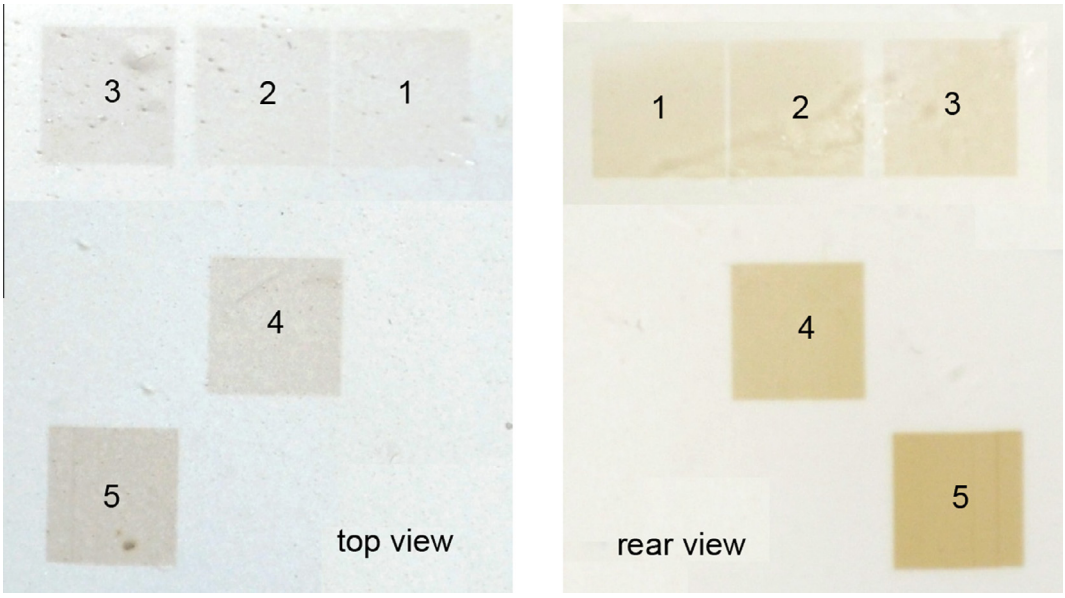

Fig. 3. Front and rear view of the model paint layer irradiated with various values of low fluences from 2.5 to 40 μC/cm^2, as in referred in Table 2. Damage starts to appears at 2.5 μC/cm^2, and is more marked on the rear view through the glass slide, where the end of the range can be observed.

might thus be actually more pronounced than observed at the surface.

The effect of low fluences at 3-MeV was investigated (1.25–40 μC/cm^2). The picture of the irradiated areas is shown in Fig. 3 and the corresponding CIE $L^*a^*b^*$ coordinates are given in Fig. 4. For the lowest value (1.25 μC/cm^2) no optical modification could be observed. A faint colour change was noted at 2.5 μC/cm^2 (area #1 in Fig. 3 and Table 2). The measured L^*a^*b values correspond to a combination of darkening (strong decrease of L^*) and a shift of hue towards yellow (increase of b^*). Interestingly, the brownish stain induced in the pigment/binder model under the same conditions appeared markedly darker than in the lead white pigments alone (hydrocerussite and cerussite pellets). This increased sensitivity was attributed to the presence of the linseed oil.

Although a relative fading of the marks could be observed over time, those induced above 10 μC/cm^2 were still visible two years after irradiation. Most important is the observation of blisters appearing a few tens of seconds after the passage of the proton beam (Fig. 5). This surface deformation was ascribed to the release of gas resulting from the binder decomposition, likely due to radiolysis, reinforced by the fact that the glass slide has prevented the escape of the gas through the back.

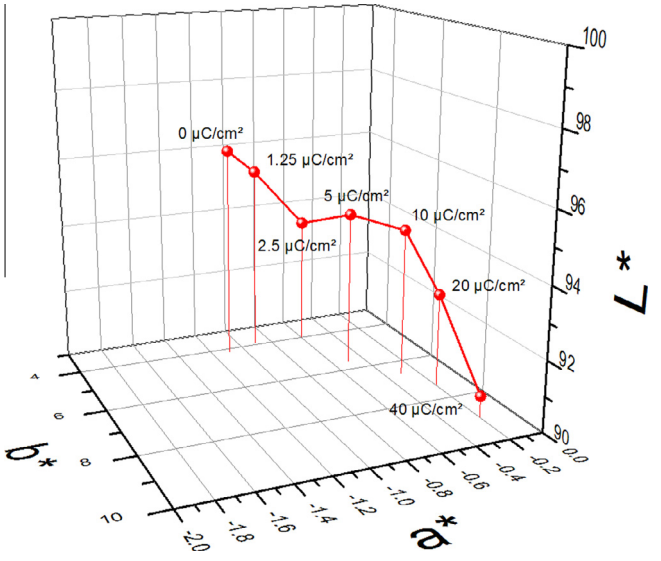

Fig. 4. Evolution of $L^*a^*b^*$ coordinates with irradiation of the model paint layer.

4.3. Ancient easel painting

Damage tests were carried out on a 19th century portrait acquired by the C2RMF for testing purposes, including sacrificial ones. The objective was to investigate the behaviour of an ancient and dry paint layer containing lead white, which can differ from that of the fresh model paint layer considered above. Indeed, it can take years to decades for an oil paint layer to dry in depth. A lead white-rich area (flesh tone) was irradiated under three fluences (10, 40 and 80 μC/cm^2). For the lowest value (10 μC/cm^2), no colour variation or physical modification of the paint surface could be evidenced (Fig. 6). At higher fluences (40 and 80 μC/cm^2) deformations in form of swelling grew under the passage of the beam, with a different aspect from the blisters induced in the model paint layers. The heights of the protrusions varied from 20 μm at 40 μC/cm^2 to 50 μm at 80 μC/cm^2 (Fig. 7, left). As shown the photomicrograph of the cross-section of the area irradiated at 80 μC/cm^2 (Fig. 7, right), the swelling of the paint layer is due the formation of microscopic bubbles, probably through the same mechanism as for the model layers, transforming the compact lead white paint layer into a foamy material with a volume expansion. Surprisingly, while the model paint layer developed a brownish mark under the beam, the irradiated areas of the ancient painting had a tendency to go white. This whitening might originate from the modification of the optical properties of the binder or the varnish, possibly opacification. Anyhow, these measurements confirm

Table 2
Colour modification induced by low fluences in the model paint layer made of lead white pigment and linseed oil. ΔE is the measured Euclidian distance between CIE $L^*a^*b^*$ coordinates.

Area #	1	2	3	4	5
Fluence (μC/cm^2)	2.5	5.4	10.8	21.6	43.5
Mean current (nA)	0.5	0.4	1.0	1.7	4.3
ΔE compared to non irradiated	1.6	2.3	3.2	6.0	7.4

Please cite this article in press as: T. Calligaro et al., PIXE analysis of historical paintings: Is the gain worth the risk?, Nucl. Instr. Meth. B (2015), http://dx.doi.org/10.1016/j.nimb.2015.08.072

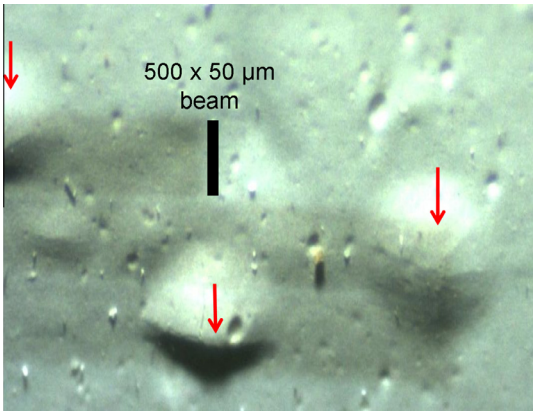

Fig. 5. Development of blisters of several hundreds of µm growing a few seconds after the passage of the beam with a fluence of 21.6 µC/cm^2 (area #4 in Table 2). A faint darkening can also be observed.

that the alteration of organic constituents (varnish, binder) is probably the most important issue when analysing paintworks using PIXE. On the other hand, the studied ancient paintings seem less sensitive than fresh paint layers (alteration arising only above 10 µC/cm^2 compared to 1.25 µC/cm^2).

5. Comparison between PIXE and XRF elemental mappings on an ancient painting

In order to assess the capabilities of the PIXE mapping, a large area (140 mm × 50 mm) of an unattributed 19th century copy of *La Bohémienne* by Frans Hals (c. 1581–1666) from the Louvre museum was scanned using both PIXE and MA-XRF (Fig. 8). The PIXE scan was carried out using the scanning system developed at AGLAE that allows scans up to 200 × 200 mm^2 with high resolution in a single pass [39]. The selected area included the face (flesh tones) which mainly contains lead-white, thus potentially most prone to beam damage. Experimental conditions were 3-MeV protons, 5 nA beam intensity, 0.2 mm pixel size, 700 × 250 pixels, 0.04 s dwell time. The total integrated charge was 35 µC, corresponding to a fluence of 0.5 µC/cm^2, thus 20 times less than the value found safe for the test painting above-reported and half of the fluence found totally non-damaging for the fresh model paint layers. PIXE spectra were recorded using three 50-mm^2 SDD detectors placed at 20 mm distance with 100-µm beryllium absorbers, with a mean count rate of 1.5 10^5 counts/s (three times 5 10^4 count/s). The scanning of the same area using MA-XRF was performed using a prototype developed at the C2RMF [40] which can record XRF elemental maps on paintings with a resolution of 0.5 mm on areas up to 300 × 300 mm^2. Operating conditions were the following: Mo tube, 40 kV, 1 mA, beam diameter 0.7 mm, 200 × 70 pixels of 0.7 mm, 0.5 s dwell time. XRF spectra were recorded using a single 25-mm^2 SDD detector, 15 mm working distance, with an average count rate of 4 × 10^4 counts/s. Note that the total time for the PIXE and MA-XRF scans were the same, namely 2 h.

The comparison of two total spectra obtained in PIXE and XRF (Fig. 9), shows that, even if one pushes aside the higher PIXE statistics due the combined use of three detectors, the balance is clearly in favour of PIXE for all elements whose lines lie below 8 keV. One can note for instance the recording of the phosphorus line at 2 keV. Even after normalization to the same number of counts in the lead L lines, a gain between 8 and 30 is noted for elements below iron (Table 3). This stems from the fact that, contrary to XRF, PIXE production yield rises with decreasing target atomic number.

The comparison of the recorded elemental maps is quite instructive (Fig. 10, the XRF maps on the left column and the PIXE maps on the right column). First, the resolution of the images obtained by PIXE (700 × 250 points) is much finer than the image recorded in the same time by XRF (200 × 70 points). This gain stems from the smaller size of the proton beam, but also from its rapid scanning using steering coils, compared to the fixed X-ray beam in XRF. Due to a lower resolution, each pixel in the XRF maps contains more counts (six times), but this is counterbalanced by the above-mentioned gain below 10 keV. The finer mercury (vermillion) and calcium PIXE maps allow to distinguish the artist's brushstrokes, which barely appears in XRF maps. The correspondence between zinc and barium in PIXE maps highlighted the use of lithopone (pigment composed of $BaSO_4$ and ZnS employed in the 19th century), with fine details around the eyes. In addition, the higher PIXE peak areas of lines below 10 keV allowed to evidence elements invisible in XRF maps: cobalt-based blue pigment in the pupils (below LOD in XRF) and phosphorus (poorly excited in XRF). The correlation between calcium and phosphorus PIXE maps highlights the use of "bone black", a black pigment obtained from burnt animal bones ($CaPO_4$). The two last outcomes were impossible to obtain using MA-XRF. The negative image of the log value of calcium in PIXE (bottom map in Fig. 10) clearly show that the painter employed bone black on a lead white background to produce the fine modelling and shading of the Bohémienne's face. Finally,

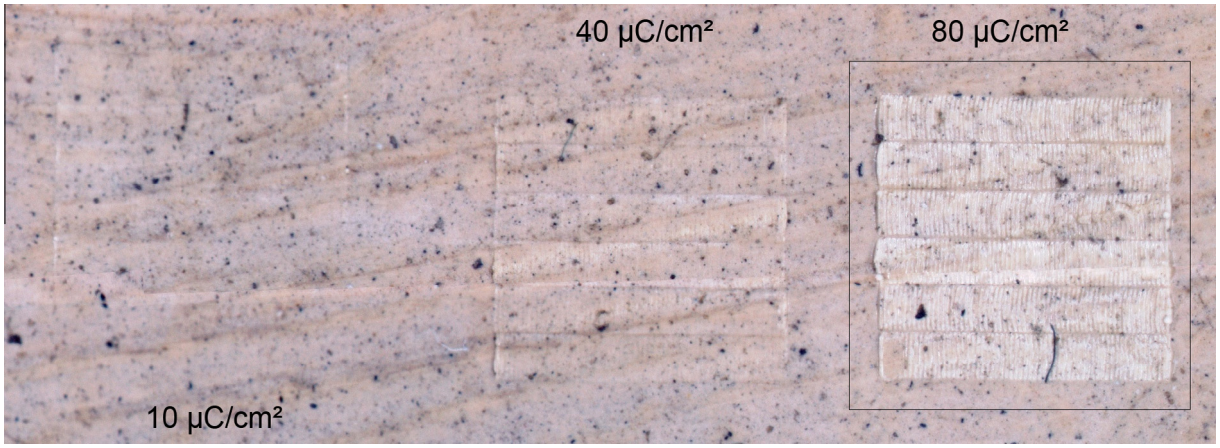

Fig. 6. Photomicrograph of the 3 × 3 mm^2 painting areas irradiated at fluences of 10, 40 and 80 µC/cm^2, left to right). On the two leftmost areas white stripes following the beam scanning can be noted.

Please cite this article in press as: T. Calligaro et al., PIXE analysis of historical paintings: Is the gain worth the risk?, Nucl. Instr. Meth. B (2015), http://dx.doi.org/10.1016/j.nimb.2015.08.072

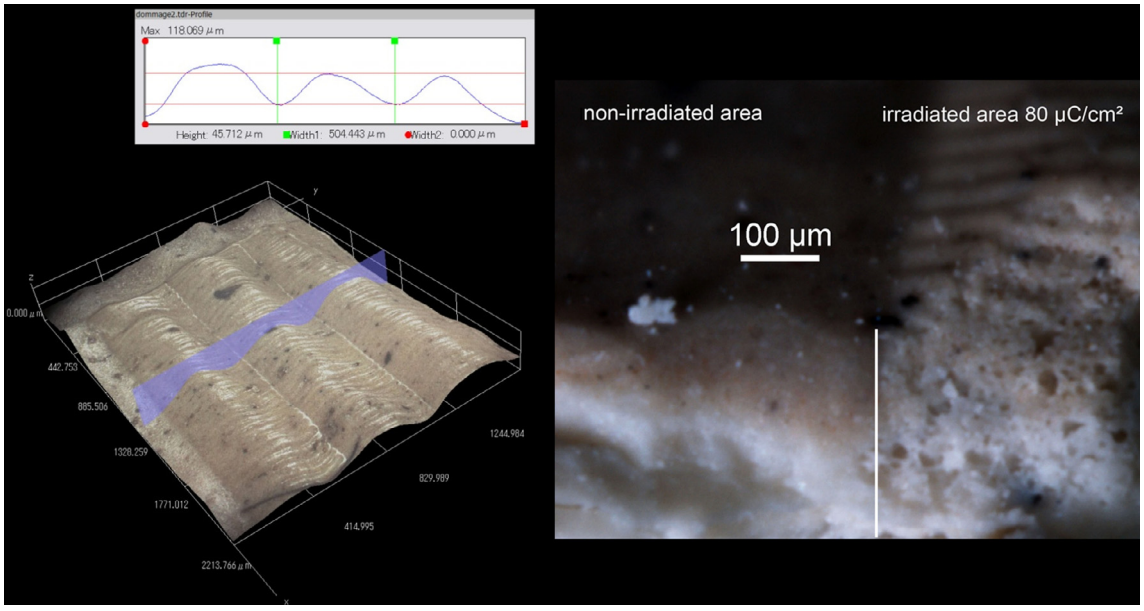

Fig. 7. Surface deformation of a painting area irradiated at 80 µC/cm^2 measured by 3D digital microscopy. On the left, the 3D view shows a vertical deformation reaching up to 50 µm. On the right, the photomicrograph of a cross section of the non-irradiated and irradiated areas shows that the swelling is due to the formation of gas bubbles.

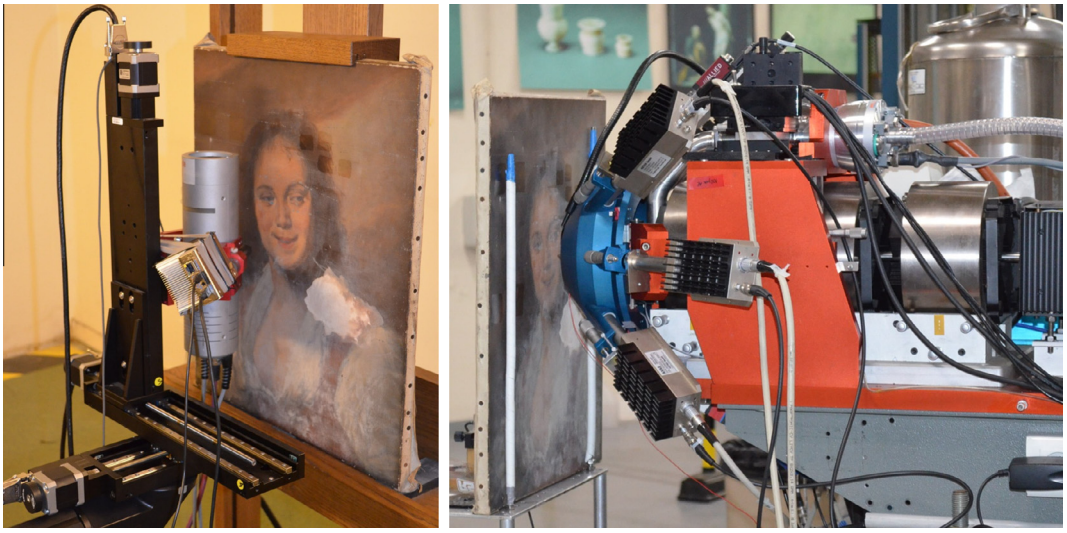

Fig. 8. Ancient painting (19th century copy of *La Bohémienne* by F. Hals, Musée du Louvre) placed in front of the MA-XRF (left) and the external PIXE scanning system (right).

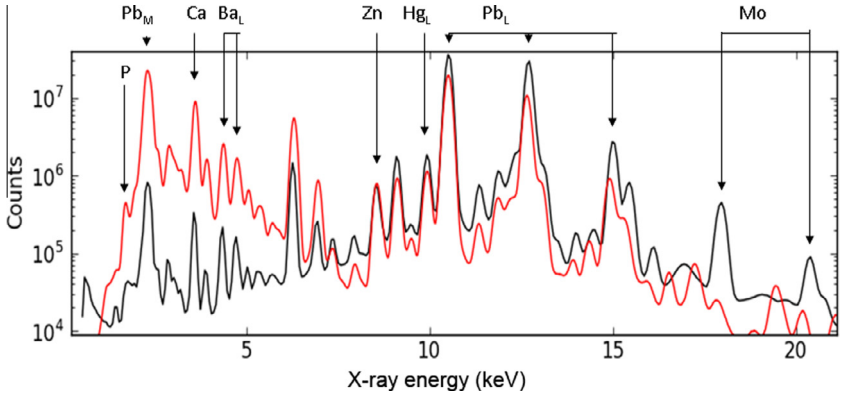

Fig. 9. Comparison of total X-ray spectra of *La Bohémienne* recorded in PIXE mapping (in red) and MA-XRF (in black). Note the improved yield for elements below 10 keV for PIXE, and the presence of phosphorus peak at 2 keV. (For interpretation of the references to colour in this figure legend, the reader is referred to the web version of this article.)

Please cite this article in press as: T. Calligaro et al., PIXE analysis of historical paintings: Is the gain worth the risk?, Nucl. Instr. Meth. B (2015), http://dx.doi.org/10.1016/j.nimb.2015.08.072

Table 3
Number of counts in the characteristics peaks of the total spectra recorded during the PIXE and XRF scans. The PIXE yields a gain between 8 and 30 for elements below Fe.

	Pb M	Ca	Fe	Pb L	Total
PIXE counts	2.5×10^8	6.0×10^7	2.5×10^7	2.2×10^8	1.0×10^9
XRF counts	2.5×10^6	6.0×10^5	3.0×10^6	1.2×10^8	3.0×10^8
Gain	$\times$ 30	$\times$ 30	$\times$ 8	$\times$ 1	$\times$ 30

a careful examination of the painting surface after irradiation did not reveal any degradation. The analytical conditions retained (0.5 μC/cm^2) have thus permitted a totally safe PIXE mapping of a large area of an ancient painting within a reasonable time.

6. Conclusions and perspectives

The PIXE technique possesses strong assets for the analysis of paintings by delivering complementary information to standard techniques like XRF. Thanks to the proton beam versatility, PIXE can provide layer profiling and large area elemental maps. As demonstrated on a real painting, PIXE mapping is complementary and possibly superior to MA-XRF, enabling to measure more efficiently elements with lines below 10 keV with an almost photographic resolution. The use of PIXE is worth provided the risk of damage is mitigated by the use of a beam fluence low enough to preserve the fragile materials in paintworks. The most sensitive pigment is probably lead white, in which hydrocerussite was found more susceptible to marking than cerussite, with dependence upon crystallite size. But the most fragile constituents are clearly the organic ones, in particular the binder (oil in the present case), whose damage is irreversible. Investigations on lead white paint layers and the ancient paintings show that below 1 μC/cm^2, as employed in previous PIXE paint studies, no alteration is observed. If one considers this fluence as a safe limit, a harmless single point PIXE analysis using 1-mm^2 diameter beam of 3-MeV protons could be obtained, for example, using a proton beam of 0.1 nA in 100 s. Using a 50-μm external micro-beam with the same intensity, the limit is reached after 0.25 s. A strategy for external PIXE mapping

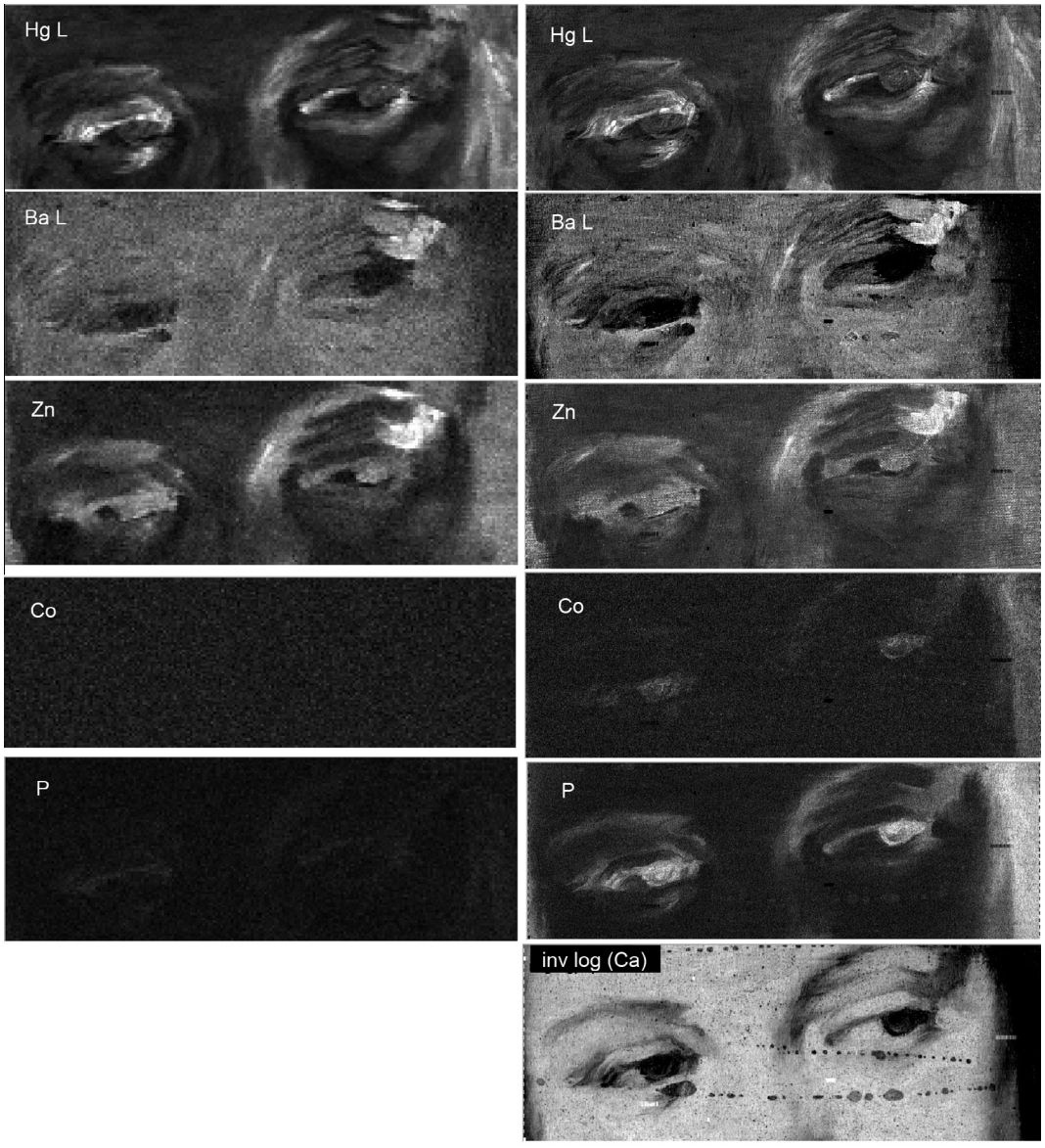

Fig. 10. Comparison of XRF elemental maps (left) and PIXE elemental maps (right). Bottom image is the PIXE map of calcium represented in negative, log scale. The Co and P maps in XRF did not show valuable information.

Please cite this article in press as: T. Calligaro et al., PIXE analysis of historical paintings: Is the gain worth the risk?, Nucl. Instr. Meth. B (2015), http://dx.doi.org/10.1016/j.nimb.2015.08.072

at 100-μm resolution complying with the 1 μC/cm^2 fluence limit would be, for instance, to scan the beam rapidly (25 pixels/s, 0.5 mm^2/sec) with a 0.04 s dwell time using a rather high current (5 nA) in order to collect enough counts in each pixel spectrum. In such conditions, a 120 × 120 mm^2 (1200 × 1200 pixels) area would be mapped in 8 h, each pixel spectrum containing several thousands of counts.

The present work focused on lead white areas, in which dark marks can more readily noticed, but evidently the behaviour of other fragile pigments and of different binders must be also considered. The preliminary studies that we carried on the verdigris organometallic pigment (copper acetate) showed a similar sensitivity to that of lead white. The varnish layer is another fragile component, but this a less an issue as it is often replaced during restorations thus seldom the original one. To our experience, historical paintings are often investigated on the occasion of restorations where varnish is removed or lightened, and that would represent a suitable opportunity for PIXE analysis. A joint research activity is currently setup in the frame of the IPERION-CH European program [41] aiming at developing damage mitigation strategies for analysis of cultural heritage materials using high radiation fluxes (particle accelerators, synchrotrons or lasers). This will offer an opportunity to develop and generalise the exploratory approach presented here, and to convince cultural heritage stakeholders that PIXE is worth and can be applied safely.

Acknowledgements

We wish to express our gratitude to the AGLAE team Dr. C. Pacheco, B. Moignard, Q. Lemasson for their skilful assistance during the PIXE experiments. Many thanks to Dr. E. Ravaud for providing the test paintings and G. Bastian for the advices on the paint layer preparation. We acknowledge the access to the EPR equipment and the interpretation of the recorded spectra by Pr. D. Gourier and Dr. Y. Le Du. We are grateful to Dr. J.-C. Dran for the revision of the manuscript and to Dr. L. Beck for important suggestions. Finally, we are indebted to Pr. P. Mandò for his precious advices and highlighting review remarks. This work was carried out in the frame of the NewAGLAE project (EQUIPEXn °2011-EQ1-22, French Ministry of Research).

References

[1] T. Calligaro, J.-C. Dran, 'Art and Archaeology applications', Chapter 12, in: M. Nastasi, J.W. Mayer, Y. Wang (Eds.), Ion Beam Analysis, Principles and Applications, Taylor and Francis Books Inc., 2014, p. 265.
[2] Jean-Claude Dran, Thomas Calligaro, AIP Conf. Proc. 1530 (2013) 11.
[3] P.A. Mandò, Nucl. Instr. Meth. B85 (1994) 815.
[4] M. Massi, L. Giuntini, M. Chiari, N. Gelli, P.A. Mandò, Nucl. Instr. Meth. B190 (2002) 276.
[5] Jean-Claude Dran, Joseph Salomon, Thomas Calligaro, Philippe Walter, Nucl. Instr. Meth. B219–220 (2004) 7.
[6] J. Salomon, J.-C. Dran, T. Guillou, B. Moignard, L. Pichon, P. Walter, F. Mathis, Nucl. Instr. Meth. B266 (2008) 2273.
[7] L. Giuntini, Anal. Bioanal. Chem. 401 (2011) 785.
[8] Pierre. Midy, Yvan. Brissaud, Nucl. Instr. Meth. B103 (1995) 489.
[9] Ivan. Brissaud, Gérard. Lagarde, Pierre. Midy, Nucl. Instr. Meth. B117 (1996) 179.
[10] I. Brissaud, A. Guilló, G. Lagarde, P. Midy, T. Calligaro, J. Salomon, Nucl. Instr. Meth. B155 (1999) 447.
[11] W. Wagner, C. Neelmeijer, Fresenius J. Anal. Chem. 353 (1995) 297.
[12] M.E. Fedi, M. Chiari, L. Giuntini, F. Lucarelli, P.A. Mandò, Nucl. Instr. Meth. B189 (2002) 56.
[13] P.A. Mandò, M.E. Fedi, N. Grassi, A. Migliori, Nucl. Instr. Meth. B239 (2005) 71.
[14] N. Grassi, A. Migliori, P.A. Mandò, H. Calvo del Castillo, X-Ray Spectrom. 34 (2005) 306.
[15] N. Grassi, P. Bonanni, C. Mazzotta, A. Migliori, P.A. Mando, X-Ray Spectrom. 38 (2009) 301.
[16] Ž. Šmit, M. Uršič, P. Pelicon, T. Trček-Pečak, B. Šeme, A. Smrekar, I. Langus, I. Nemec, K. Kavkler, Nucl. Instr. Meth. B266 (2008) 2047.
[17] G. Weber, J.M. Delbrouck, D. Strivay, F. Kerff, L. Martinot, Nucl. Instr. Meth. B139 (1998) 196.
[18] H.W. Lefevre, R.M. Schofield, D.R. Ciarlo, Nucl. Instr. Meth. B54 (1991) 47.
[19] T. Calligaro, J.-C. Dran, J. Salomon, Ph. Walter, Nucl. Instr. Meth. B226 (2004) 29.
[20] L. de Viguerie, L. Beck, J. Salomon, L. Pichon, Ph. Walter, Anal. Chem. 81 (19) (2009) 7960.
[21] L. Beck, L. de Viguerie, Ph. Walter, L. Pichon, P.C. Gutiérrez, J. Salomon, M. Menu, S. Sorieul, Nucl. Instr. Meth. B268 (2010) 2086.
[22] L. Beck, C. Jeynes, N.P. Barradas, Nucl. Instr. Meth. B266 (2008) 1871.
[23] C. Neelmeijer, I. Brissaud, T. Calligaro, G. Demortier, A. Hautojärvi, M. Mäder, L. Martinot, M. Schreiner, T. Tuurnala, G. Weber, X-Ray Spectrom. 29 (2000) 101.
[24] G. Demortier, A. Adriaens (Eds.), Ion Beam Study of Art and Archaeological Objects, a contribution by members of the COST G1 Action, European Commission, Luxembourg (2000) EUR 19218.
[25] Annemie Adriaens, Guy Demortier, Nucl. Instr. Meth. B226 (2004) 3.
[26] Matthias Alfeld, José A.C. Broekaert, Spectrochim. Acta B88 (2013) 211.
[27] Matthias Alfeld, Joana Vaz Pedroso, Margriet van Eikema Hommes, Geert Van der Snickt, Gwen Tauber, Jorik Blaas, Michael Haschke, Klaus Erler, Joris Dik, Koen Koen, J. Anal. At. Spectrom. 28 (2013) 760.
[28] M. Alfeld, K. Janssens, J. Dik, W. de Nolf, G. van der Snickt, J. Anal. At. Spectrom. 26 (2011) 899.
[29] L. Giuntini, M. Massi, S. Calusi, Nucl. Instr. Meth. A576 (2007) 266.
[30] P.A. Mandò, M.E. Fedi, N. Grassi, Eur. Phys. J. Plus 126 (2011) 41.
[31] Novella. Grassi, Nucl. Instr. Meth. B267 (2009) 825.
[32] Loïc Bertrand, Sebastian Schöeder, Demetrios Anglos, Mark B.H. Breese, Koen Janssens, Mehdi Moini, Aliz Simon, TrAC, Trends Anal. Chem. 66 (2015) 128.
[33] Alessandro Zucchiatti, Fernando Agulló-Lopez, Nucl. Instr. Meth. B278 (2012) 106.
[34] J. Absil, H.-P. Garnir, D. Strivay, C. Oger, G. Weber, Nucl. Instr. Meth. B198 (2002) 90.
[35] O. Enguita, T. Calderón, M.T. Fernández-Jiménez, P. Beneitez, A. Millan, G. García, Nucl. Instr. Meth. B219–220 (2004) 53.
[36] L. Beck, P.C. Gutiérrez, F. Miserque, L. Thomé, Nucl. Instr. Meth. B307 (2013) 20.
[37] R.J. Gettens, H. Kühn, W.T. Chase, Stud. Conserv. 12 (4) (1967) 125.
[38] M. Stols-Witlox, L. Megens, L. Carlyle, To prepare white excellent... Reconstructions investigating the influence of washing and grinding of stack-process lead white on pigment composition and particle size, Archetype Publications Ltd., London, 2012, p. 112. ISBN: 978-1-904982-73-9.
[39] L. Pichon, B. Moignard, Q. Lemasson, C. Pacheco, P. Walter, Nucl. Instr. Meth. B318 (2014) 27.
[40] Myriam Eveno, Elisabeth Ravaud, Thomas Calligaro, Laurent Pichon, Eric Laval, Heritage Sci. 2 (2014) 17.
[41] <http://www.iperionch.eu/iperion-vision> (07-2015).